The construction of olfactory representations

Thomas A. Cleland

Dept. of Psychology
Cornell University
Ithaca, NY 14853

+1-607-255-8099 voice
+1-775-254-2756 fax
tac29@cornell.edu

Chapter 11 in: Hölscher C, Munk M (2008) Mechanisms of information processing in the brain: information processing in neuronal populations. Cambridge, UK: Cambridge University Press.

Abstract

The simple model of sensory systems as passive recorders of external stimuli is giving way to a richer understanding of how sensory systems actively sample their environment and parse the complex and often degenerate signals embedded in the resulting primary sensory representations. In the vertebrate olfactory system, much of the relevant neural processing occurs within the olfactory bulb, a discrete, highly structured cortical network that receives direct projections from primary sensory neurons and projects in turn to several different cortical and subcortical targets. The rate-coded activity of these primary sensory neurons is selective for different aspects of odor quality (structural motifs on odorant molecules), but the quality of this signal is unavoidably limited by additive and antagonistic interference among ambient odorants as well as multiple sources of confounding variance. In contrast, bulbar output activity is sparse and temporally structured, and reflects not only material stimulus quality but also the learned contingency of meaningful odors. I present a two-stage cascade theory of olfactory bulb stimulus processing that integrates across levels of analysis to describe the transformations in both form and content of these seriate olfactory representations.

Introduction

Sensory information progresses centrally from the primary sensors in the periphery to the central neural structures that derive relevant environmental information from these sensory data and determine appropriate physiological and behavioral responses. In this chapter, I present a general theory of early olfactory sensory processing in the primary olfactory epithelium and olfactory bulb (OB). The theory depicts olfactory sensory processing as a cascade of representations, each of which exhibits characteristic physical properties and is sampled by appropriate neural mechanisms in order to construct the subsequent representation. The primary olfactory representation is mediated by the activation pattern across the population of primary olfactory sensory neurons (OSNs) in the sensory epithelium. The secondary olfactory representation is similarly mediated by the activation pattern across the population of principal neurons immediately postsynaptic to the OSNs, known as mitral cells. (Mitral cell axons diverge dramatically, projecting to roughly ten different central structures within the brain; the resulting tertiary and subsequent olfactory representations are constructed outside the olfactory bulb and are not discussed at length herein). The transformation between the primary and secondary representations is a robust, intricate, two-stage process that corrects for artifacts that can hinder the recognition of odor qualities, regulates stimulus selectivity, and transduces the underlying mechanics from a robust but costly rate-coding scheme on a slow respiratory (theta-band) timescale to a sparse dynamical representation operating on the beta- and gamma-band timescales and suitable for integration with other central neural processes. Odor memory mechanisms within the OB, dynamical coordination with central structures,

and the regulation of sampling behaviors all modulate the patterned spiking output of OB principal neurons, thereby selectively sampling and filtering afferent sensory information pursuant to the needs of the organism.

I. Stimulus encoding in olfactory sensory neurons

OSNs are embedded within a sensory epithelium that lines a portion of the nasal cavity and is covered with a layer of mucus. OSNs extend a protrusion into this mucus layer known as the dendritic knob, from which extend several cilia between 1 and 200 um in length (ciliary lengths vary both within and between species; Figure 1; (Getchell, 1986; Morrison and Costanzo, 1990, 1992)). Odorous molecules inhaled into the nose dissolve into the mucus layer and associate with the extracellular binding sites of odorant receptor proteins located on these OSN cilia. These associations trigger transduction cascades within OSNs that form the basis of the **primary olfactory representation**.

Odorant receptors (ORs) are G protein-coupled seven-transmembrane (7TM) receptors related to other 7TM proteins such as rhodopsin and β-adrenergic receptors (Buck and Axel, 1991; Mombaerts, 1999). Their association with certain odorant molecules elicits a conformational change which is propagated through the plasma membrane, releasing intracellular G proteins which, in turn, activate membrane-associated adenylate cyclase enzymes that generate the second messenger cyclic AMP (cAMP). One target of this cAMP is a cyclic nucleotide-gated (CNG) ion channel permeant to sodium and calcium ions, the opening of which depolarizes the OSN. The activation of calcium-dependent chloride channels by this influx of calcium – the third messenger – magnifies the evoked

potential by enabling the efflux of chloride ions into the chloride-poor mucus, potentiating the depolarization of the OSN. There are specific subclasses of OSN that utilize a cGMP-based transduction cascade instead (Meyer et al., 2000), and other transduction mechanisms may also play a role (Restrepo et al., 1990; Kaur et al., 2001), but the principle is the same: odorant binding evokes a cascade response in OSNs that can be dramatically amplified by the second- and third-messenger cascades that it activates. The resulting depolarization of the OSN evokes a train of action potentials, the frequency of which depends systematically on the intensity of the odor-evoked depolarization (Getchell and Shepherd, 1978; Rospars et al., 2000). These spike trains are temporally unsophisticated and (as is typical for primary sensory neurons across modalities) are generally considered to be simple **rate codes** reporting the intensity of activation of the corresponding sensory neuron, modulated to a moderate extent by intracellular adaptation processes that serve to emphasize transient changes in the intensity of activation (Zufall and Leinders-Zufall, 2000).

Elemental odor stimuli

In a formal sense, essential for a quantitative understanding of olfactory processing, the elemental odor stimulus is not an odorant molecule *per se*, but rather "that aspect of an odorant molecule that associates with a single type of odorant receptor" or even "the net effect of a given odorant molecule on a single type of odorant receptor." This theoretical element has been termed an odor epitope, or **odotope** (the term *odotope* is preferable as it does not connote a literal correspondence with molecular structural features), and reflects the fact that, just as any given OR can bind to many different odorant molecules, single

odorant molecules also bind to (and activate) many different ORs. It is important for theoretical purposes to dissociate the abstract odotope concept from the physical binding sites on odorant molecules from which it is derived; for example, increasing the concentration of an odorant will increase the number of odotopes binding at significant levels to their corresponding ORs, but one would not say that a given odotope comes to associate with more than one OR type. The fact that a given molecular structural feature may associate with multiple ORs and hence contribute physically to multiple odotopes is not relevant at this level of analysis, nor is the fact that the precise balance of ligand-receptor associations that constitute each odotope (i.e., that contribute to the net activation of a given OR by a single given odorant) will change with concentration. In this odotopic parlance, the intricate matrix of associations between odorant structural features and ORs reduces to the simple statement that *odorant molecules are comprised of a characteristic combination of odotopes, each of which associates with a specific OR.*

The association of odotopes with their receptors is described by standard pharmacological laws; indeed, a number of "puzzling" problems in olfaction are simple corollaries of these laws. Ligand-receptor binding is described by rate constants for association and dissociation, yielding sigmoidal (or sums-of-sigmoidal) binding curves that depict the equilibrium probability (or proportion) of ligand-receptor association as a function of ligand concentration. The ligand concentration at which 50% association is achieved is the dissociation constant (K_d), a measure of ligand-receptor **affinity**. The maximum slope of the binding curve (also at 50% association) determines the Hill coefficient, or cooperativity, of the reaction. (Odotope-receptor associations that exhibit multiple affinities yield more complex, sums-of-sigmoidal binding curves, but the

underlying principle is the same). Of equally critical importance is a separate term, **efficacy**, which describes the effectiveness of the odotope – once bound to the OR – at activating the OSN transduction cascade. Affinity and efficacy are distinct properties; for example, an odotope with high affinity and low efficacy represents a receptor antagonist that will not be directly detected by the olfactory system when presented alone but which can interfere with the ability of other, simultaneously-presented odorants to activate that OR. While this phenomenon is predictable from first principles it has only recently been explicitly described in the olfactory system (Araneda et al., 2004; Oka et al., 2004).

The deployment of metabotropic 7TM receptors as ORs enables a further dissociation between the ligand-receptor binding curve *per se* and the analogous dose-response curve of cellular activation. Specifically, the decoupling of the 7TM receptor from its effector ion channels enables a receptor with a modest binding affinity to a given ligand to mediate a cellular response of arbitrarily high sensitivity to the presence of that ligand (Figure 2). Furthermore, the degree of functional sensitivity can be smoothly regulated by the modulation of intracellular cascades or the differential deployment of receptor and effector populations, enabling a population of OSNs expressing the same type of odorant receptor (and hence possessing identical receptive fields) to be differently tuned for concentration. A convergent population of such neurons will collectively express an arbitrarily broad dose-response function, much like those observed in OB glomeruli (see below), without distorting the receptive field. This model (Cleland and Linster, 1999) both explains the extreme sensitivity exhibited by some animals' olfactory systems without relying on implausibly strong ligand-receptor affinities and resolves the conundrum of how the collective dose-response curves measured by glomerular imaging (and in mitral cell

responses) can be rendered substantially broader than those measured in individual OSN recordings. These principles illustrate the sophistication of odor representation at even the most peripheral levels, suggesting how OSN properties may be organized so as to take advantage of physical laws to increase their collective coding capacity and reduce the computational burden on subsequent processing stages.

Defining the odotope as the elemental odor stimulus offers several critical advantages to quantitative analysis. The association of each odotope with its receptor exhibits a characteristic set of ligand-receptor binding constants. Indeed, as noted above, it is likely that a given odotope-receptor association will have multiple sets of binding constants, each with a characteristic efficacy, although it suffices for most purposes to model these complex odotope-receptor interactions as a single sigmoidal binding function with a single efficacy. The primary sensory representation of an odorant molecule presented at a given concentration, then, is simply the sum of the primary representations of its constituent odotopes at that concentration. The problem of representing odor mixtures is also conceptually simplified. From an odotopic perspective, single odorant molecules *are* mixtures (of odotopes); combinations of multiple odorant molecules are conceptually no different. However, the concentrations of odotopes associated with different odorant molecules may now vary with respect to one another, and multiple odotopes (associated with different odorant molecules) may now compete for the same receptor. As odotopes by definition associate with a single OR type, computing these competitive interactions is elementary. The primary representation of complex mixtures, rendered as an intractable, recursive problem from the perspective of odorant molecules, is thereby reduced to a conceptually simple list of independent competitive interactions. The problem of

"subtractive" interactions, for example, in which particular OSNs respond less to a mixture of A+B than they do to A alone (at the same concentration), is explained as a simple matter of competition between a high-efficacy odotope for that receptor contained in A and a low-efficacy odotope of comparable affinity contained in B.

An odotopic basis for quantifying odor representations also renders tractable the problem of the dimensionality of odor space. Whereas primary auditory stimuli can be mapped along the single dimension of frequency, and visual stimuli can be retinotopically mapped in two dimensions, the similarity spaces in which olfactory stimuli can be mapped are irreducibly high-dimensional. Furthermore, unlike frequency or distance, the axes of variation among chemical stimuli themselves cannot be unambiguously identified, much less rendered orthogonal to one another. As with the definition of the odotope, which utilizes the population of expressed ORs to organize the stimulus properties of odorant molecules, the solution lies in the inclusion of sensor properties within the definition of the sensory space. Specifically, each axis of variation is defined as the activation level of a single OR type; hence, the dimensionality of odor space is identical to the number of different OR types expressed (roughly 350 in humans, 1000 in mice; (Mombaerts, 1999, 2001)). These axes should be construed as orthogonal, in that each OR type can in principle be independently activated. This orthogonality principle is made clear by studies employing "artificial odor" stimuli via the direct electrical stimulation of glomeruli (Mouly et al., 1990; Mouly et al., 1993), in which any combination of OR-specific elemental stimuli can be administered, and holds despite the fact that, in any finite odor environment, consistent correlations will be measurable between the activation levels of particular ORs. A capacity for orthogonality is also important to ensure that the olfactory system is

appropriately responsive in diverse odor environments, as the statistics of odorant prevalence have a strong impact on measures of elemental similarity.

An odotopic basis function for odor representation significantly disambiguates and simplifies the representation and quantification of odor stimuli. It is explicitly species-specific in that it depends quantitatively on the complement of ORs expressed by a given subject; hence, phenomena such as the overlap between two odor representations cannot be directly compared between two species that may express different OR complements. While this is clearly appropriate and does not constitute a weakness in the odotopic approach for its intended purpose, odotopic depictions of odorant similarity consequently are of limited value outside of a biological context.

OSN receptive fields

Stimulus selectivity in the olfactory system is primarily generated by the diversity of ORs that are expressed among the OSN population. Different populations of OSNs express different ORs that are responsive to different odotopes, such that the representation of any given odor arises from the degree to which its constituent odotopes bind to their cognate ORs and activate particular subpopulations of OSNs. Hence, a given odor, presented at a given concentration and in the absence of background odors or other disruptive stimuli, evokes a characteristic, replicable profile of activation across the set of all such OSN subpopulations. This stimulus specificity at the primary receptor level in olfaction offers a potent advantage (over, for example, vision) to computational studies of sensory processing, because the basis for the perception of stimulus quality is derived directly from the **receptive fields** of primary OSNs. The quantification of olfactory

receptive fields (also known as *molecular receptive ranges*; (Mori and Shepherd, 1994)), however, exhibits challenges similar to those encountered in the definition of elemental odor stimuli, which can be met by adherence to the following principles:

(1) The receptive field of a neuron must be defined in terms of the output activity that different odor stimuli elicit in that neuron, rather than ligand-receptor binding *per se*. For present purposes, receptive fields will be defined as that range of stimuli that evoke a net excitatory response in a neuron. For principal neurons such as OSNs and mitral cells, "output" implies the evocation of action potentials. Hence, a stimulus evoking an excitatory synaptic input to a neuron that is overcome by simultaneous heterosynaptic inhibition such that the neuron produces no action potentials will not be considered part of that neuron's receptive field. Similarly, an odor that does not activate a given neuron is not part of that neuron's receptive field even if some of its component molecules activate that neuron when presented separately.

(2) The receptive fields of neurons must be considered as distinct from the receptive fields of the receptors that they express. Hence, an OSN expressing two types of odorant receptor would have a single receptive field combining those of both receptors. Similarly, the receptive fields of central neurons must be considered independently of the receptive fields of neurons presynaptic to them, as the transfer function between the two is highly stimulus-dependent and can be arbitrarily complex.

(3) Receptive fields are dynamic and contextual properties that may vary with stimulus intensity (odorant concentration), centrifugal neuromodulation, mixture properties, or a number of other factors. Experimental measurements of receptive fields also depend,

of course, on the range of test stimuli used to probe them, and hence will nearly always yield underestimates of their scope.

This framework for defining olfactory receptive fields clarifies some idiosyncratic olfactory phenomena for theoretical purposes, two examples of which follow. First, canonically, in mammals, each OSN expresses exactly one OR – indeed, in mice, allelic inactivation ensures that only one of the two alleles of each OR is expressed (Chess et al., 1994; Strotmann et al., 2000). All other OR genes in that cell are silenced. However, this strict pattern of one OR per OSN is not uniformly exhibited in all species, some of which appear to express multiple OR types in a single OSN; even in mammals it is not certain that this pattern is strictly maintained (Mombaerts, 2004). This indicates that the one-OR-per-OSN property is not a critical feature of the olfactory system, but a variant with (presumably) some species-specific utility. Indeed, while the expression of only one OR per OSN (and just one allele thereof) renders the receptive fields of individual OSNs as narrow as can be achieved solely by regulating OR expression, it does not qualitatively affect the nature of the neural computation. OSNs expressing any complement of receptors will exhibit a single, overall receptive field. The formation of narrower receptive fields through highly selective receptor expression and/or allelic inactivation is simply one strategy with characteristic costs and benefits; specifically, sensors with narrower receptive fields can improve the capacity of the olfactory system to discriminate among highly similar odorants, but require deployment of a greater number of differently-tuned sensors in order to remain comparably sensitive to the same range of different odors. Indeed, the one-receptor-type-per-OSN strategy was identified in mice, which are macrosmatic

mammals expressing large numbers of different OR species. In the nematode *Caenorhabditis elegans* and the fruit fly *Drosophila melanogaster*, in contrast, recent work indicates that this principle is not strictly respected (Troemel et al., 1995; Goldman et al., 2005).

Second, it often has been suggested that ORs exhibit uniquely broad receptive fields among 7TM receptors, based on the well-known sensitivity of OSNs and ORs to a reasonably broad range of odor ligands. There is as yet no valid reason to believe that this is true. All receptors in general, and 7TM receptors in particular, are sensitive to any ligand able to induce their reconformation into the active state. Multiple agonists, weak agonists, and weak and strong antagonists have been identified for all well-studied receptor species (although typically only strong agonists and strong antagonists become widely known because of their experimental utility). The primary functional difference between the receptive fields of odorant receptors and other 7TM receptors is not a property of the receptor *per se*, but of the statistical structure of their normal stimulus environments. Most receptors are embedded in a highly regulated environment in which only a single effective agonist is normally present, hence establishing their nominal status as "glutamate receptors" or "acetylcholine receptors" largely on the basis of that limited environment. The actual receptive field of β_1-adrenergic receptors, for example, is considerably broader, including epinephrine, norepinephrine, isoproterenol, xamoterol, and denopamine as full agonists, whereas the inhibitory surround (antagonists) includes alprenolol, propranolol, pindolol, betaxolol, and atenolol. Odorant receptors, in contrast, are deployed directly into the unregulated chemical environment of the external world, wherein the scope and

complexity of their receptive fields cannot be functionally overlooked, and indeed is essential to their function in that context.

Olfactory sensory neuron convergence

OSN axons project via the olfactory nerve to synapse with mitral cells and multiple classes of interneurons within the olfactory bulb (OB), a telencephalic cortex devoted to the processing of olfactory sensory information. Critically, the axons of OSNs expressing the same OR converge together, intertwining their axonal arbors within the surface layer of the OB to form **glomeruli** (singular: **glomerulus**). Glomeruli are surrounded by glia (and hence visible as spheroid structures under the light microscope, particularly in mammals) and contain no cell bodies. Mitral cells (the principal neurons of the OB), as well as multiple classes of periglomerular and tufted cells, extend dendrites into one or a few glomeruli, wherein they receive synaptic inputs from OSN axons and from one another. In particular, mitral cells in mammals tend to sample strictly from a single glomerulus, although – like the one-OR-per-OSN hypothesis – this principle is not strictly adhered to across species, illustrating another advantage of treating mitral cell receptive fields independently from those of their presynaptic OSNs. Interestingly, most classes of bulbar interneurons – at least in mammals – also confine the majority of their synaptic interactions to single glomeruli and their associated mitral cells, such that the olfactory bulb exhibits a **columnar** chemotopic structure. There are several exceptions to this, of course, notably the short-axon cells of the deep glomerular layer (Aungst et al., 2003) and the sparse axons of periglomerular cells. Interestingly, even granule-mitral interactions, previously an

obvious counterexample to this generalization about OB columns, now appear to adhere to this columnar organization (Willhite et al., 2006).

The selective clustering into glomeruli of the axon terminals of OSNs expressing the same OR, irrespective of the locations of their somata within the nasal epithelium, is the single most important feature of OSN convergence. The convergence of OSNs with similar receptive fields enables the promulgation of chemoselectivity to subsequent OB processing layers, as coordinated neural computations can be performed across populations of similarly tuned neurons, in principle improving both coding capacity and odor sensitivity (van Drongelen et al., 1978; Duchamp-Viret et al., 1989; Cleland and Linster, 2005) as well as extending the range of concentrations across which consistent representations can be maintained (Cleland and Linster, 1999). Moreover, the clustering of thousands of similarly-tuned axonal arbors into discrete regions (glomeruli) transforms the surface of the olfactory bulb into a visualizable map of the activation levels of each OR-specific OSN type expressed. This phenomenon has been an experimental windfall; visualization of glomerular activity across the OB surface using any of a number of techniques enables direct measurement of the primary olfactory representation – that is, of the population-average activation levels of each OR-specific population of OSNs.

Degenerate feature maps of odor stimulus qualities

The patterns of glomerular activity recorded by such imaging techniques constitute degenerate odotopic feature maps. That is, for a single odorant presented at a single concentration they are specific to and diagnostic for the presence of that odorant, being composed of a map of the relative efficacies of all the odotopes comprising that odorant.

Increasing the concentration of an odorant, however, damages this characteristic relational activity pattern by recruiting new glomeruli into the active ensemble and increasing the activity of existing glomerular signals (generally but not necessarily monotonically) until a maximum is reached, as is predictable by the law of mass action for increasing ligand concentrations. Furthermore, the simultaneous presence of multiple odorants typically results in competition between their odotopes for access to certain ORs, the result of which may be anywhere from fully additive (summation) to subtractive (blockade), introducing significant ambiguity into the combined representation. As most common odors – such as the smell of apples or green grass – are comprised of dozens to hundreds of odorant species in characteristic ratios, and will nearly always be perceived in the presence of simultaneous unrelated but comparably complex odor sources (cow manure, baking bread), the degeneracy of complex odor representations imposes a critical limitation on sensory processing. Indeed, such limitations substantially define the perceptual problems that downstream sensory processing must solve and constrain the computational mechanisms that it can effectively use.

A second important constraint on chemosensory processing mechanisms is the lack of an ordered topography of stimulus quality across the OB surface, which limits the mechanisms that can be deployed to perform **similarity-dependent computations** on the primary representation – that is, processes such as contrast enhancement that rely upon a representation of the similarities among stimuli in their inputs. Olfactory contrast enhancement clearly occurs at the level of mitral cells (Yokoi et al., 1995), despite the fact that, as discussed above, the similarities among odorant stimuli are distributed high-dimensionally. While the choice of basis function for this distribution is essentially

arbitrary, the minimum dimensionality of an odor representation in an unrestricted or unpredictable chemosensory environment is equal to the number of differentiable sensors (i.e., the number of different OR types); in any species this number is substantially greater than two. This latter point is critical, as a dimensionality greater than two precludes the representation of stimulus similarity by physical proximity within cortical or other layered neural structures (Kohonen, 1982; Kohonen and Hari, 1999; Cleland and Sethupathy, 2006). Hence, there can be no olfactory analogue to the frequency maps observed along the cochlea or inferior colliculus, nor to the two-dimensional retinotopic map of visual space. The physical location of glomeruli can not and does not connote the chemoselective properties of their associated ORs. This does not imply that all glomeruli are distributed randomly with respect to their chemoselectivity – data regarding putatively activity-dependent glomerular segregation (Ishii et al., 2001; Tozaki et al., 2004) and sensitivity to whole-molecule properties (Schoenfeld and Cleland, 2005, 2006) provide two counterexamples – but it does mean that neighborhood relationships among glomeruli are not reliable bases for the neural representation of stimulus similarity. Because of this, nearest-neighbor synaptic projections will not reliably target neurons with correspondingly similar receptive fields; consequently, despite efforts to argue the contrary, similarity-dependent computations such as olfactory contrast enhancement cannot be mediated by proximity-dependent mechanisms such as nearest-neighbor lateral inhibition in the olfactory system (Cleland and Sethupathy, 2006). This property places additional major constraints on bulbar processing mechanisms, as discussed below.

II. Stimulus processing in the olfactory bulb

Despite the many computational operations deployed in OSNs and in the architecture of their convergence, these are only the beginnings of the sensory processing cascade. Highly redundant rate coding on a slow **timescale**, as exhibited by the OSN population, is advantageous to primary olfactory sampling but also extraordinarily inefficient and metabolically costly (Attwell and Laughlin, 2001). (Timescale in this context refers to *precision*, i.e., the degree of variance in spike timing tolerated in a neuron before the meaning of its signal is altered from the perspective of a given follower). Central cortical representations and processing mechanisms, in contrast, are sparse and timing-sensitive on considerably faster timescales than populations of isolated OSNs can support. Hence, the information contained in the primary olfactory representation must be transformed to become physically compatible with the processing rules and architecture of the cerebral cortex. Furthermore, OSN receptive fields are unregulated beyond that which is inherent in OR structure. Features of odor stimulus quality are not fully disambiguated from artifacts of concentration, nor are the responses to odotopes associated with different odorants (or odors) disambiguated from one another so that they can be appropriately identified or learned. The centrifugal regulatory influences of selective attention, perceptual learning, and the like have had little or no capacity to influence stimulus processing. Hence, in addition to the physical transformation, the afferent representation must be integrated with descending and neuromodulatory influences as well as locally situated memory effects. This process begins in the olfactory bulb.

The OB is a multi-layered telencephalic cortical structure. While it contains a substantial diversity of cell types interconnected within an intricate synaptic architecture (Figure 3A), and much remains to be learned about its capacities, it can be rendered relatively tractable for study by emphasizing two of its architectural properties. First, the same mitral (and middle/deep tufted) principal neurons that are directly postsynaptic to OSNs constitute the only output of the OB network. Consequently, all bulbar processing converges onto one target effector: the pattern of spikes generated by these principal neurons. Second, synaptic inputs onto mitral cells within the OB are located in one of two discrete regions: either within the glomerular layer (OSNs, external tufted cells, GABAergic and dopaminergic periglomerular cells) or within the external plexiform layer (*EPL*; granule cells). Centrifugal descending and neuromodulatory inputs affecting mitral cells also generally conform to these two regions, or else exert their effects indirectly by influencing interneurons. These principles frame the following presentation of OB function.

Glomerular computations

The first processing stage for OSN spike trains entering the OB is within the glomerular layer itself. OSNs form synapses not only onto mitral cell dendrites, but also onto two classes of interneuron: periglomerular cells and external tufted cells. The former are GABAergic and dopaminergic inhibitory interneurons that inhibit mitral cells via a $GABA_A$-ergic mechanism as well as presynaptically inhibiting OSN terminals with $GABA_B$ or dopamine D2 pharmacology. The latter are glutamatergic excitatory interneurons that synapse onto periglomerular cells and one another as well as with another

class of glomerular-layer interneurons known as short-axon cells. Critically, these two cell types mediate the only two feed-forward sources of afferent information that can modify mitral cell activity. In contrast, feedback circuits such as mitral-granule lateral interactions in the EPL depend on mitral cell activation as the sole source of afferent input by which to modify mitral cell firing properties. Consequently, the strengths and capabilities of the glomerular and EPL networks differ substantively, as illustrated below.

Despite their direct innervation by OSNs, the most common response of mitral cells to odor stimuli is inhibition. While odor-inhibited mitral cells are often excited by direct OSN inputs, their concomitant inhibition by periglomerular cells coactivated by the same odor stimuli shunts this excitation and prevents spike generation. Theoretical models demonstrate that glomerular circuitry is well suited for this function (Cleland and Sethupathy, 2006). OSN inputs to periglomerular cells occur in the same tiny spines that are presynaptic to mitral cell dendrites (Figure 3B; (Pinching and Powell, 1971)); the electrotonic compactness and high input resistance of these spines performs a much more potent current-to-voltage transformation than does the considerably larger mitral cell dendrite, enabling this disynaptic pathway to exert its inhibitory effect upon the depolarizing mitral cell dendrite comfortably before the latter can initiate spiking (as demonstrated by the prevalence of inhibitory odor responses in mitral cells and the observation of early transient hyperpolarizations even in excited mitral cells; (Hamilton and Kauer, 1989; Kauer et al., 1990; Wellis and Scott, 1990)). The question then becomes: under what circumstances does the direct excitation of mitral cells overpower this inhibitory influence so as to initiate spiking? The most parsimonious hypothesis is that it is a simple matter of input strength. That is, while weak and moderate inputs result in the

inhibition of mitral cells, the capacity of this inhibitory circuit saturates, such that stronger odor stimuli generate excitatory inputs that overpower the concomitant inhibition, depolarizing the mitral cell and evoking action potentials (Figure 4A). This mechanism has two great strengths. First, it results in an improved relational representation, as the mitral cells sampling from the strongest-activated glomeruli (those with receptive fields best tuned to the stimulus) will be consistently activated while those sampling from less-specifically activated glomeruli will be inhibited out of the active ensemble. With the inclusion of global feedback circuitry, odor quality representations can be constructed in mitral cells that are largely independent of concentration (i.e., normalized; (Cleland and Sethupathy, 2006; Cleland et al., 2007)), at least on the slower timescales associated with rate coding (c. 10s-100s of ms; (Chalansonnet and Chaput, 1998)). Second, to the extent that concentration effects can be mitigated by normalization, this circuit generates a unidirectional on-center/inhibitory surround function (**half-hat function**, or half of a "Mexican hat" function; Figure 4B,C) with ligand-receptor affinity as the independent variable. By regulating the competitive efficacies of the excitatory and inhibitory influences on mitral cell activation, this critical circuit property enables regulation of the stringency of odor selectivity via contrast enhancement with respect to the high-dimensional similarity space in which odotope qualities are distributed, irrespective of the particular topology of that space (Cleland and Sethupathy, 2006). This independence from topology is an important feature, as topologies of odor similarity depend on the statistics and features of the current odor environment and hence are unpredictable. Moreover, this hypothesized mechanism of contrast enhancement requires no targeted lateral inhibitory projections (unlike the analogous operations in the visual and auditory modalities), and

hence is entirely independent of the physical location of glomeruli on the surface of the OB. In contrast to the visual and auditory modalities, location is not used as a surrogate for stimulus quality, and physical proximity does not connote similarity. As the physical distribution of chemoselective glomeruli on the bulbar surface consequently is irrelevant to the representation or processing of stimulus quality, neither normal variations in glomerular positioning (Strotmann et al., 2000) nor the experimental generation of novel glomeruli (Serizawa et al., 2000; Ishii et al., 2001; Tozaki et al., 2004) would be expected to affect the integrity of olfactory perception. This also demonstrates the critical importance of broad receptive fields among OSNs, as the ordering of different ORs' receptive fields in a high-dimensional similarity space – and hence the perception of similarity – relies upon measurable degrees of overlap.

EPL computations

The second layer of processing in the OB takes place in the external plexiform layer between the extensive lateral dendrites of mitral cells and the dendrites of inhibitory granule cells. The architecture of this interaction differs substantially from that of the glomerular synaptic network. Mitral cells are the only afferent input to the system and also comprise the only output of interest; consequently, granule cell effects on mitral cell activity are entirely dependent on feedback. Reciprocal synapses between mitral cells (excitatory) and granule cells (inhibitory) mediate lateral inhibitory interactions between mitral cells and also support synchronized field oscillations across the OB as discussed below. However, these lateral inhibitory interactions do not play the classical contrast enhancement role in olfaction that they do in other modalities. First, the granule cell

synapses mediating this inhibition are electrotonically very distant from the excitatory afferent driver currents in the distal apical dendrite, within the glomerulus, from which mitral cell spikes are initiated. As the efficacy of shunt inhibition is strongly dependent on location (Koch et al., 1983; Liu, 2004; Mel and Schiller, 2004), lateral inhibitory interactions in the EPL are poorly situated to prevent mitral cell spike initiation. (In contrast, as discussed above, intraglomerular feed-forward shunt inhibition, delivered directly to the location of OSN excitatory inputs by periglomerular spines, is ideally situated to regulate spike initiation). Furthermore, of course, mitral-granule lateral inhibition is dependent on the prior initiation of spiking activity in mitral cells, and hence cannot be the source of the initial inhibitory response of mitral cells to odor presentation that precedes even the most rapid excitatory responses (Hamilton and Kauer, 1989; Kauer et al., 1990; Wellis and Scott, 1990). These data indicate that mitral-granule interactions are not the source of the classical contrast enhancement processes that have been observed in mitral cell odor responses (Yokoi et al., 1995); in this sense, the olfactory bulb does not resemble the retina. Rather, as discussed above, this function appears to be mediated by glomerular circuitry.

Lateral inhibition among mitral cells in the EPL does, however, appear capable of influencing the timing of mitral cell spikes (David et al., ; Lagier et al., 2004; Bathellier et al., 2006; Lledo and Lagier, 2006), a function essential to its role in the dynamical synchronization properties of the OB as discussed below. However, lateral inhibition in the OB does not imply a retinal, on-center/inhibitory surround architecture; odor stimulus qualities are still mapped high-dimensionally, and lateral inhibition that is localized within a two-dimensional neighborhood cannot effectively process higher-dimensional maps.

Furthermore, the absence of parallel, feed-forward inhibitory afferent inputs in the EPL precludes the inheritance of a topology of similarity from the external environment such as occurs in the glomerular layer, because there is no physical basis by which to map the inhibitory surround. In the glomerular layer, high-dimensional processing relies upon the feed-forward interactions of one excitatory and one inhibitory process with the latter exhibiting greater sensitivity (or, equivalently, a broader receptive field at any given concentration) than the former. This information is not available to the EPL network. Hence, whereas the EPL processing layer is architecturally capable of mediating lateral inhibition in arbitrarily high dimensions – as required for useful olfactory representation and processing – it lacks a means to map this capability onto an externally-defined topology of similarity. The clear implication is that these considerable computational resources instead mediate secondary transformations on olfactory representations based not on physical stimulus attributes but rather on internally-defined combinatorial and psychological features not directly related to chemical structure, such as odor binding (Roskies, 1999; Treisman, 1999) and olfactory learning (reviewed in (Wilson and Stevenson, 2006)). Indeed, odor learning has profound effects on odor processing properties and even OB cellular architecture. Associative learning increases the prevalence of inhibitory responses by mitral cells to reinforced odor stimuli (Wilson and Leon, 1988), improves odor detection performance, and affects animals' capacities to discriminate related odorants (Fletcher and Wilson, 2002). Even nonmotivated experience with odorants reduces and re-tunes mitral cell odor responses (Buonviso et al., 1998; Buonviso and Chaput, 2000; Fletcher and Wilson, 2003), a process that may be mediated by enhanced granule cell activity coupled with effects on NMDA-dependent synaptic

connectivity (Lincoln et al., 1988; Brennan et al., 1990; Garcia et al., 1995). On a longer timescale, the survival of newly-generated granule and periglomerular cells maturing within the OB also depends on olfactory experience (Rochefort et al., 2002; Mandairon et al., 2003), and the newly-integrated neurons are distributed in an odor- and task-specific manner reflecting olfactory learning (Alonso et al., 2006; Lledo et al., 2006; Mandairon et al., 2006a). Learned associations between disparate elements of odor representations may be essential for binding the structurally unrelated components of odors into unitary phenomena; if this is indeed one of the functions of the mitral-granule network in the EPL, then it is clearly beneficial that its computational topology is not constrained by the physically-defined structural similarity of chemical odotopes that define that of the glomerular layer.

A separate problem from that of topology is, of course, mechanism. How are odor representations physically transformed by EPL computations? The emerging answer is that this second stage of olfactory stimulus processing operates in a dynamical regime, with modifications to the secondary olfactory representation mediated not by the generation or prevention of spiking but by the subtler regulation of spike timing. As with similarity mapping in the glomerular layer, physical proximity again appears to play little or no role in the topology of stimulus processing. Active membrane properties within mitral cell lateral dendrites appear to propagate excitation laterally without appreciable distance-dependent loss (Xiong and Chen, 2002; Debarbieux et al., 2003). In contrast, the effects of shunt inhibition do not propagate and consequently remain distance-dependent (David et al., ; Lowe, 2002). Indeed, it has been hypothesized that lateral signal propagation in the EPL may depend solely on nondecrementing excitation along mitral cell

lateral dendrites, whereas only those granule cell inputs nearly adjacent to the soma of any given mitral cell would deliver shunt inhibition with appreciable efficacy (Lowe, 2002; Willhite et al., 2006), so as, for example, to influence the timing of its spikes. This hypothesis is theoretically attractive for several reasons: not only does it remove the disruptive effects of physical proximity imposed by differentially located sources of shunt inhibition, it also resolves most of the combinatorial problem arising from bidirectional information transfer in mitral cell lateral dendrites, in which accumulating shunt inhibition interferes with the outgoing active propagation of excitation (Lowe, 2002). Finally, and most importantly, it suggests a columnar architecture for the organization of granule cells reflecting that of glomeruli and their associated mitral cells (Willhite et al., 2006); specifically, those granule cells physically adjacent to a given mitral cell would be associated with delivering effects onto that mitral cell, whereas mitral cell output onto granule cells would be independent of proximity. Precisely this neighborhood-independent columnar architecture has been proposed based on recent imaging work, contingent on the hypothesis that the efficiency of retrograde transmission of pseudorabies virus tracer is activity dependent or otherwise related to synaptic efficacy (Willhite et al., 2006).

If this hypothesis is correct, then what might be the function of electrotonically distant inhibitory synapses on mitral cell lateral dendrites? Reciprocal synapses between mitral and granule cells are distributed along the full length of the mitral cell lateral dendrite. One possibility is that these reciprocal synapses contribute to maintaining the synchronicity of field oscillations across the olfactory bulb, constituting a background coordinating process that is not directly relevant to odor stimulus processing. A more provocative hypothesis is that these inhibitory inputs may selectively attenuate the lateral

propagation of excitation so as to regulate the pattern of associations among activated mitral cells (Lowe, 2002). This possibility exemplifies the capacity of the EPL network to process high-dimensional representations without reference to the physical similarities among stimuli on which glomerular layer processing depends. Rather, as noted above, EPL processing is likely to reflect bulbar learning, as suggested by the dependence of these synaptic interactions on NMDA receptors (Schoppa et al., 1998; Chen et al., 2000). Indeed, both of these hypotheses may have value; calcium imaging studies have demonstrated that relatively weak mitral cell activation produces activity in granule cells that is confined to the spine, presumably minimizing the degree of lateral inhibition compared to recurrent (self-) inhibition, whereas stronger activation excites broader regions of the granule cell dendritic tree (Egger et al., 2003, 2005). The dependence of the latter on T-type calcium currents further suggests a robust, all-or-none effect.

The genesis of spike timing and synchronization

Glomerular computations yield, at first approximation, an initial pattern of activation across the array of mitral cells that is sparser in space than the primary (glomerular) representation on which it depends, owing to periglomerular cell-mediated inhibition, but similarly structured in time. Mitral cells' activity is modulated by breathing (Yokoi et al., 1995; Buonviso et al., 2006; Roux et al., 2006) and they respond with a substantial latency (100s of ms) to the presentation of odor stimuli. The roughly theta-band (in rats and mice) timescale of olfactory inputs is physically limited by the low-pass filtering properties of the inhalation cycle, the fluid mechanics of the nasal cavity, the time required for odorants to adsorb to and diffuse through the nasal mucus layer, the transduction and integration time

within OSNs, and the inhibition delay imposed by the OSN-periglomerular-mitral synaptic triad. There is no known basis for afferent olfactory information to be encoded by OSNs on any faster timescale than this.

Cortical processing, in contrast, operates at a substantially faster timescale. Cortical spiking, while sparse, is believed to be tightly regulated in time. This temporal precision is essential for the coordination of spike timing among convergent inputs to enable critical computations such as heterosynaptic facilitation, long-term potentiation, and spike-timing dependent plasticity (Song et al., 2000; Cleland and Linster, 2002). In order to integrate into the cortical signaling network, primary olfactory representations must be transformed appropriately in timescale and sparseness, and in such a way that the perceptual information of interest is retained within the resulting secondary representation (mitral cell spike patterning). This transformation occurs largely within the olfactory bulb, as mitral cell spiking is regulated on cortical timescales (Lagier et al., 2004; Lledo and Lagier, 2006) and their axons diverge to at least ten cortical and subcortical destinations (Cleland and Linster, 2003). The mechanisms underlying the transformation of the slow-timescale primary representation to the fast-timescale secondary representation appear to arise from a combination of endogenous OB properties and descending inputs, according to the following theoretical model.

Mitral cells are intrinsically resonant in the beta band, exhibiting intrinsic subthreshold oscillations at a frequency dependent upon the membrane potential (from 10 Hz at –67 mV to as high as 40 Hz at –59 mV). Inhibitory inputs to mitral cells reset the phase of these oscillations, whereas the effects of excitatory inputs are modulated by the oscillatory phase such that mitral cell spiking output is phase-constrained (Desmaisons et al., 1999; Rubin

and Cleland, 2006). These properties are remarkably potent when framed in the general model of the OB synaptic triad presented above. Olfactory input, presented to odor receptors synchronously at the slower (theta-band) timescale of inhalation, evokes a potent inhibition in all mitral cells postsynaptic to activated OSNs, thereby synchronizing the phases of their intrinsic oscillations. A subset of these mitral cells – those sampling from the most strongly activated glomeruli – then overcome this inhibition and fire action potentials. The timing of these action potentials is phase-constrained by the intrinsic membrane properties of the mitral cells, all of which are transiently phase-locked by the preceding inhibitory pulse. The net effect is twofold: first, the initial ensemble of mitral cell spiking is regulated on a roughly beta-band timescale rather than the theta (or slower) band of the inhalation-exhalation cycle. Second, the distribution of spikes within the first resulting phase window is likely to be ordered by the intensity of activation of the mitral cells that generate them, essentially because stronger inputs yield shorter-latency spikes. Hence, at first approximation, the intensity of activation of each glomerulus is likely to be reflected not in the intensity of mitral cell activation, but in the timing of the first spikes evoked by the corresponding mitral cells (White et al., 1992; Hopfield, 1995; Cleland and Linster, 2002). Indeed, just this pattern is observable in mitral cell responses to increasing odorant concentrations: higher concentrations tend to evoke shorter spike latencies in cells that respond to a given odorant presentation with excitation, although this effect becomes conflated with other factors in extended concentration series and hence is not a universal rule. Furthermore, using timing-dependent synaptic facilitation and learning rules, many common neural computations such as contrast enhancement can be performed in this timing-dependent, dynamical regime (Figure 5; (Linster and Cleland, 2001; Cleland and

Linster, 2002)). In sum, according to this working model, the initial stimulus-dependent response across the mitral cell population consists of a relatively sparse active ensemble that is dependent on odor quality but substantially independent of concentration, with the relative intensities of activation of neurons within this phase-constrained ensemble encoded by spike precedence.

Mitral-granule oscillogenesis

Sustained gamma-band oscillations within the olfactory bulb are credited with constraining mitral cell spike times and maintaining a coordinated clock across the mitral cell ensemble (Kashiwadani et al., 1999). The origin and mechanisms underlying these oscillations are complex and under investigation, but they certainly depend on reciprocal interactions between the lateral dendrites of mitral cells and the dendrites of inhibitory granule cells within the EPL (Schoppa, 2006b), and are closely coordinated with oscillatory processes in central olfactory structures such as the piriform cortex (Bressler et al., 1993; Kay and Freeman, 1998). (During certain phases of olfactory learning, these intrinsic gamma oscillations give way to centrally-coordinated beta-band oscillations, reviewed by Lledo and Lagier (2006), which will not be discussed in detail herein). Several network models have been proposed to underlie OB intrinsic oscillatory properties. Generally, these models are based on an excitatory-inhibitory oscillator mechanism by virtue of the prominent mitral-granule reciprocal synapses present in the OB (Li and Hopfield, 1989; Eeckman and Freeman, 1990), although alternative models have been presented that emphasize different characteristic properties of the OB network. In particular, models based on mutual synaptic inhibition may more robustly exhibit the

independence of oscillatory frequency from input intensity that is observed in the OB (Linster and Gervais, 1996), and are lent credence by evidence that disruption of GABA receptors specifically located on granule cells affects the oscillatory properties of the OB (Nusser et al., 2001) and by the recent description of a source for GABAergic inputs to granule cells (granule-granule synapses are experimentally contraindicated): a population of OB interneurons known as Blanes cells (Pressler and Strowbridge, 2006; Schoppa, 2006a). Alternatively, or additionally, GABAergic projections from the basal forebrain (Zaborszky et al., 1986) may play a role.

Despite the ongoing debate regarding dynamical mechanisms, it is clear that OB field oscillations are dependent on coordinated mitral-granule synaptic interactions, and that disruption of these interactions influences perception (e.g., (Nusser et al., 2001)) as first shown in the analogous insect system (Stopfer et al., 1997). However, coordinated network oscillations are slower to arise from inputs that are disorganized in time than from inputs that are all relatively synchronous. The phase resetting and spike-time constraining properties of the glomerular synaptic triad coupled with mitral cell intrinsic resonance properties appear to initiate OB oscillations efficiently and replicably, bypassing an indeterminate period of poorly coordinated activity in the OB network preceding its settlement into a synchronized state, and hence improving reaction times and preventing the loss of potentially critical sensory information. Just as the theta-band coordination among OSNs due to respiration is essential for priming the beta-band synchronization of the onset of mitral cell spiking, so is this transient beta-band coordination essential for the rapid transition to gamma-band spike synchronization among mitral cells.

Active sampling, neuromodulation, and natural scenes

Deeper aspects of neural representations also can feed back onto sensory processing. Centrifugal neuromodulation of the OB – presumably mediating attention, motivation, and other aspects of behavioral state – is a prominent regulator of olfactory perception (Linster and Cleland, 2002; Yuan et al., 2003; Mandairon et al., 2006b), and OB gamma-band oscillations are coordinated with those of other cortices and also depend on behavioral state (Kay and Freeman, 1998; Kay and Laurent, 1999; Kay, 2003; Ravel et al., 2003; Martin et al., 2004; Martin et al., 2006). Furthermore, odor-sampling behavior itself (sniffing) is behaviorally modulated; some effects of sniffing behavior on odor representations may optimize sampling based on anatomical specializations (Schoenfeld and Cleland, 2006), while others appear more temporally sophisticated, suggesting that a more detailed exploration of the interactions among timescales in this complex system is warranted. In particular, repeated active sniffing generates a nonstationary series of odor representations (Spors et al., 2006), potentially providing additional mechanisms for odor discrimination or identification.

The final frontier in olfactory stimulus processing is odor segmentation, or the identification of a relevant odor despite its conflation with other environmental odorants. There is no *a priori* reason why a particular combination of odotopes should be treated as a single stimulus, much less when the characteristic odotope ratios that might identify an odorant are degraded by the simultaneous presence of other odorants incorporating odotopes that compete for the same ORs. While efforts have been made to create feedforward models of odor segmentation, these have by and large been unenlightening. It is likely that the solution to mixture processing and odor segmentation relies critically on

olfactory memory to identify and segregate learned representations from the olfactory milieu, though the mechanisms that may underlie such a process are far from clear. Study of the properties of tertiary olfactory representations in the piriform cortex (Illig and Haberly, 2003; Kadohisa and Wilson, 2006; Linster et al., 2006) and other postbulbar structures (Haberly, 2001; Lei et al., 2006), as well as of OB interactions with putative associative memory networks (Haberly and Bower, 1989; Barkai et al., 1994), will be necessary in order to shed light on the neural mechanisms underlying segmentation and the putative OB contribution to the process.

Summary: The two-stage cascade hypothesis of OB stimulus processing

Sensory processing can be understood as a cascade of sequential representations, each with characteristic properties and mechanisms that contribute to the construction of the subsequent representation. As described herein, two sequential odor representations and two stages of processing are contained within the OB; subsequently, the great divergence of mitral/tufted cell axons implies that on the order of ten separate – and potentially quite different – tertiary representations will be constructed in different regions of the brain (Cleland and Linster, 2003), although among these by far the greatest attention has been paid to the piriform cortex. A consistent model of OB processing and information content is hence an important prerequisite to the considerably larger problem of higher-order sensory processing across the brain. The following model is proposed as a framework for understanding and quantifying OB computational processing.

The primary olfactory representation is constructed across the OSN population – the primary olfactory sensory neurons – and reflected in the glomerular maps across the OB

input layer that are dominated by OSN axonal arbors. Several cellular and network specializations facilitate the consistent sampling of the odor environment – mitigating intensity differences, emphasizing environmental changes – and set the stage for subsequent processing. The resulting primary representation is based on a highly redundant rate code (in other words, a slow timescale) and hence is energetically costly. As with primary sensory neurons in general, this is probably a necessary adaptation to its function, in which unpredictable time-varying stimulus properties are likely to dominate any attempt at fast-timescale temporal control, but it also introduces the need to transform the representation into a more energetically efficient representation compatible with other cortical signaling rules.

The secondary olfactory representation – the patterned spiking output of the OB – is a remarkable transformation of the primary representation. It is sparser in its use of spikes, temporally precise on a markedly faster timescale, robust to the disruptive effects of concentration variance, and integrates afferent sensory processing with centrifugal descending and neuromodulatory influences. The construction of the secondary representation is mediated by intricate neural computations that can be grouped into two stages with markedly different features. The first stage takes place in the glomerular layer. It operates directly on OSN output activity and hence is characterized by effects on a slower timescale (theta-band or slower) consistent with OSN rate coding. Effective inhibition implies the prevention of spiking in mitral/tufted cells, and effective activity is judged largely by *whether* spikes are evoked (equivalently, *when* on a slow timescale). This first stage of processing is feed-forward, operates in a topology of similarity defined by the external chemical environment and mediated by the overlap in OR receptive fields,

and specifically includes computations that rely upon the grouping or differentiation of structurally similar stimulus features. The second stage is mediated in the EPL and is based on dynamical interactions between mitral and granule cells. It operates on mitral cell activation profiles and acts to influence activity in those same mitral cells, and hence is based on feedback. Owing to mitral cell intrinsic resonance properties that elevate the timescale to beta-band and mitral-granule synaptic dynamical properties that further elevate it to gamma-band, the timescale of the secondary representation is considerably faster than that of the primary representation, while spiking is rendered concomitantly sparser, in part due to the normalization of concentration effects. Effective inhibition implies the delay of mitral cell spiking, and effective mitral cell activity is judged by *when* – on a millisecond timescale – spikes are evoked. EPL processing is potentially high-dimensional, as is glomerular processing, but owing to its feedback architecture the EPL topology is isolated from the externally-defined similarity space that defines glomerular processing. Consequently, it remains free to support arbitrary associations among OB columns, which appear to reflect odor experience and olfactory learning and may contribute to complex processing such as the binding of multiple features into unitary odor percepts. In sum, the OB is a sophisticated sensory parsing engine, transforming sensory representations in form, bias and context so that they can be usefully integrated into the global operations of the central nervous system and thereby serve the needs of the organism.

References

Alonso M, Viollet C, Gabellec MM, Meas-Yedid V, Olivo-Marin JC, Lledo PM (2006) Olfactory discrimination learning increases the survival of adult-born neurons in the olfactory bulb. J Neurosci 26:10508-10513.

Araneda RC, Peterlin Z, Zhang X, Chesler A, Firestein S (2004) A pharmacological profile of the aldehyde receptor repertoire in rat olfactory epithelium. J Physiol 555:743-756.

Attwell D, Laughlin SB (2001) An energy budget for signaling in the grey matter of the brain. J Cereb Blood Flow Metab 21:1133-1145.

Aungst JL, Heyward PM, Puche AC, Karnup SV, Hayar A, Szabo G, Shipley MT (2003) Centre-surround inhibition among olfactory bulb glomeruli. Nature 426:623-629.

Barkai E, Bergman RE, Horwitz G, Hasselmo ME (1994) Modulation of associative memory function in a biophysical simulation of rat piriform cortex. J Neurophysiol 72:659-677.

Bathellier B, Lagier S, Faure P, Lledo PM (2006) Circuit properties generating gamma oscillations in a network model of the olfactory bulb. J Neurophysiol 95:2678-2691.

Brennan P, Kaba H, Keverne EB (1990) Olfactory recognition: a simple memory system. Science 250:1223-1226.

Bressler SL, Coppola R, Nakamura R (1993) Episodic multiregional cortical coherence at multiple frequencies during visual task performance. Nature 366:153-156.

Buck L, Axel R (1991) A novel multigene family may encode odorant receptors: a molecular basis for odor recognition. Cell 65:175-187.

Buonviso N, Chaput M (2000) Olfactory experience decreases responsiveness of the olfactory bulb in the adult rat. Neuroscience 95:325-332.

Buonviso N, Amat C, Litaudon P (2006) Respiratory modulation of olfactory neurons in the rodent brain. Chem Senses 31:145-154.

Buonviso N, Gervais R, Chalansonnet M, Chaput M (1998) Short-lasting exposure to one odour decreases general reactivity in the olfactory bulb of adult rats. Eur J Neurosci 10:2472-2475.

Chalansonnet M, Chaput MA (1998) Olfactory bulb output cell temporal response patterns to increasing odor concentrations in freely breathing rats. Chem Senses 23:1-9.

Chen WR, Xiong W, Shepherd GM (2000) Analysis of relations between NMDA receptors and GABA release at olfactory bulb reciprocal synapses. Neuron 25:625-633.

Chess A, Simon I, Cedar H, Axel R (1994) Allelic inactivation regulates olfactory receptor gene expression. Cell 78:823-834.

Cleland TA, Linster C (1999) Concentration tuning mediated by spare receptor capacity in olfactory sensory neurons: A theoretical study. Neural Comput 11:1673-1690.

Cleland TA, Linster C (2002) How synchronization properties among second-order sensory neurons can mediate stimulus salience. Behav Neurosci 116:212-221.

Cleland TA, Linster C (2003) Central olfactory processing. In: Handbook of olfaction and gustation, 2nd ed. (Doty RL, ed), pp 165-180. New York: Marcel Dekker.

Cleland TA, Linster C (2005) Computation in the olfactory system. Chem Senses 30:801-813.

Cleland TA, Sethupathy P (2006) Non-topographical contrast enhancement in the olfactory bulb. BMC Neurosci 7:7.

Cleland TA, Johnson BA, Leon M, Linster C (2007) Relational representation in the olfactory system. Proc Natl Acad Sci U S A In press.

David F, Linster C, Cleland TA Lateral dendritic shunt inhibition can regularize mitral cell spike patterning. Submitted to J Comput Neurosci.

Debarbieux F, Audinat E, Charpak S (2003) Action potential propagation in dendrites of rat mitral cells in vivo. J Neurosci 23:5553-5560.

Desmaisons D, Vincent JD, Lledo PM (1999) Control of action potential timing by intrinsic subthreshold oscillations in olfactory bulb output neurons. J Neurosci 19:10727-10737.

Duchamp-Viret P, Duchamp A, Vigouroux M (1989) Amplifying role of convergence in olfactory system a comparative study of receptor cell and second-order neuron sensitivities. J Neurophysiol 61:1085-1094.

Eeckman FH, Freeman WJ (1990) Correlations between unit firing and EEG in the rat olfactory system. Brain Res 528:238-244.

Egger V, Svoboda K, Mainen ZF (2003) Mechanisms of lateral inhibition in the olfactory bulb: efficiency and modulation of spike-evoked calcium influx into granule cells. J Neurosci 23:7551-7558.

Egger V, Svoboda K, Mainen ZF (2005) Dendrodendritic synaptic signals in olfactory bulb granule cells: local spine boost and global low-threshold spike. J Neurosci 25:3521-3530.

Fletcher ML, Wilson DA (2002) Experience modifies olfactory acuity: acetylcholine-dependent learning decreases behavioral generalization between similar odorants. J Neurosci 22:RC201.

Fletcher ML, Wilson DA (2003) Olfactory bulb mitral-tufted cell plasticity: odorant-specific tuning reflects previous odorant exposure. J Neurosci 23:6946-6955.

Garcia Y, Ibarra C, Jaffe EH (1995) NMDA and non-NMDA receptor-mediated release of [3H]GABA from granule cell dendrites of rat olfactory bulb. J Neurochem 64:662-669.

Getchell TV (1986) Functional properties of vertebrate olfactory receptor neurons. Physiol Rev 66:772-818.

Getchell TV, Shepherd GM (1978) Responses of olfactory receptor cells to step pulses of odour at different concentrations in the salamander. J Physiol 282:521-540.

Goldman AL, Van der Goes van Naters W, Lessing D, Warr CG, Carlson JR (2005) Coexpression of two functional odor receptors in one neuron. Neuron 45:661-666.

Haberly LB (2001) Parallel-distributed processing in olfactory cortex: new insights from morphological and physiological analysis of neuronal circuitry. Chem Senses 26:551-576.

Haberly LB, Bower JM (1989) Olfactory cortex: model circuit for study of associative memory? Trends Neurosci 12:258-264.

Hamilton KA, Kauer JS (1989) Patterns of intracellular potentials in salamander mitral/tufted cells in response to odor stimulation. J Neurophysiol 62:609-625.

Hopfield JJ (1995) Pattern recognition computation using action potential timing for stimulus representation. Nature 376:33-36.

Illig KR, Haberly LB (2003) Odor-evoked activity is spatially distributed in piriform cortex. J Comp Neurol 457:361-373.

Ishii T, Serizawa S, Kohda A, Nakatani H, Shiroishi T, Okumura K, Iwakura Y, Nagawa F, Tsuboi A, Sakano H (2001) Monoallelic expression of the odourant receptor gene and axonal projection of olfactory sensory neurones. Genes Cells 6:71-78.

Kadohisa M, Wilson DA (2006) Olfactory cortical adaptation facilitates detection of odors against background. J Neurophysiol 95:1888-1896.

Kashiwadani H, Sasaki YF, Uchida N, Mori K (1999) Synchronized oscillatory discharges of mitral/tufted cells with different molecular receptive ranges in the rabbit olfactory bulb. J Neurophysiol 82:1786-1792.

Kauer JS, Hamilton KA, Neff SR, Cinelli AR (1990) Temporal patterns of membrane potential in the olfactory bulb observed with intracellular recording and voltage-sensitive dye imaging: early hyperpolarization. In: Chemosensory information processing (Schild D, ed), pp 305-314. Berlin: Springer-Verlag.

Kaur R, Zhu XO, Moorhouse AJ, Barry PH (2001) IP3-gated channels and their occurrence relative to CNG channels in the soma and dendritic knob of rat olfactory receptor neurons. J Membr Biol 181:91-105.

Kay LM (2003) Two species of gamma oscillations in the olfactory bulb: dependence on behavioral state and synaptic interactions. J Integr Neurosci 2:31-44.

Kay LM, Freeman WJ (1998) Bidirectional processing in the olfactory-limbic axis during olfactory behavior. Behav Neurosci 112:541-553.

Kay LM, Laurent G (1999) Odor- and context-dependent modulation of mitral cell activity in behaving rats. Nat Neurosci 2:1003-1009.

Koch C, Poggio T, Torre V (1983) Nonlinear interactions in a dendritic tree: localization, timing, and role in information processing. Proc Natl Acad Sci U S A 80:2799-2802.

Kohonen T (1982) Self-organized formation of topology correct feature maps. Biol Cybern 43:59-69.

Kohonen T, Hari R (1999) Where the abstract feature maps of the brain might come from. Trends Neurosci 22:135-139.

Lagier S, Carleton A, Lledo PM (2004) Interplay between local GABAergic interneurons and relay neurons generates gamma oscillations in the rat olfactory bulb. J Neurosci 24:4382-4392.

Lei H, Mooney R, Katz LC (2006) Synaptic integration of olfactory information in mouse anterior olfactory nucleus. J Neurosci 26:12023-12032.

Li Z, Hopfield JJ (1989) Modeling the olfactory bulb and its neural oscillatory processings. Biol Cybern 61:379-392.

Lincoln J, Coopersmith R, Harris EW, Cotman CW, Leon M (1988) NMDA receptor activation and early olfactory learning. Brain Res 467:309-312.

Linster C, Gervais R (1996) Investigation of the role of interneurons and their modulation by centrifugal fibers in a neural model of the olfactory bulb. J Comput Neurosci 3:225-246.

Linster C, Cleland TA (2001) How spike synchronization among olfactory neurons can contribute to sensory discrimination. J Comput Neurosci 10:187-193.

Linster C, Cleland TA (2002) Cholinergic modulation of sensory representations in the olfactory bulb. Neural Netw 15:709-717.

Linster C, Henry L, Kadohisa M, Wilson DA (2006) Synaptic adaptation and odor-background segmentation. Neurobiol Learn Mem.

Liu G (2004) Local structural balance and functional interaction of excitatory and inhibitory synapses in hippocampal dendrites. Nat Neurosci 7:373-379.

Lledo PM, Lagier S (2006) Adjusting neurophysiological computations in the adult olfactory bulb. Semin Cell Dev Biol 17:443-453.

Lledo PM, Alonso M, Grubb MS (2006) Adult neurogenesis and functional plasticity in neuronal circuits. Nat Rev Neurosci 7:179-193.

Lowe G (2002) Inhibition of backpropagating action potentials in mitral cell secondary dendrites. J Neurophysiol 88:64-85.

Mandairon N, Jourdan F, Didier A (2003) Deprivation of sensory inputs to the olfactory bulb up-regulates cell death and proliferation in the subventricular zone of adult mice. Neuroscience 119:507-516.

Mandairon N, Sacquet J, Jourdan F, Didier A (2006a) Long-term fate and distribution of newborn cells in the adult mouse olfactory bulb: Influences of olfactory deprivation. Neuroscience 141:443-451.

Mandairon N, Ferretti CJ, Stack CM, Rubin DB, Cleland TA, Linster C (2006b) Cholinergic modulation in the olfactory bulb influences spontaneous olfactory discrimination in adult rats. Eur J Neurosci 24:3234-3244.

Martin C, Gervais R, Messaoudi B, Ravel N (2006) Learning-induced oscillatory activities correlated to odour recognition: a network activity. Eur J Neurosci 23:1801-1810.

Martin C, Gervais R, Hugues E, Messaoudi B, Ravel N (2004) Learning modulation of odor-induced oscillatory responses in the rat olfactory bulb: a correlate of odor recognition? J Neurosci 24:389-397.

McQuiston AR, Katz LC (2001) Electrophysiology of interneurons in the glomerular layer of the rat olfactory bulb. J Neurophysiol 86:1899-1907.

Mel BW, Schiller J (2004) On the fight between excitation and inhibition: location is everything. Sci STKE 2004:PE44.

Meyer MR, Angele A, Kremmer E, Kaupp UB, Muller F (2000) A cGMP-signaling pathway in a subset of olfactory sensory neurons. Proc Natl Acad Sci U S A 97:10595-10600.

Mombaerts P (1999) Seven-transmembrane proteins as odorant and chemosensory receptors. Science 286:707-711.

Mombaerts P (2001) The human repertoire of odorant receptor genes and pseudogenes. Annu Rev Genomics Hum Genet 2:493-510.

Mombaerts P (2004) Odorant receptor gene choice in olfactory sensory neurons: the one receptor-one neuron hypothesis revisited. Curr Opin Neurobiol 14:31-36.

Mori K, Shepherd GM (1994) Emerging principles of molecular signal processing by mitral/tufted cells in the olfactory bulb. Semin Cell Biol 5:65-74.

Morrison EE, Costanzo RM (1990) Morphology of the human olfactory epithelium. J Comp Neurol 297:1-13.

Morrison EE, Costanzo RM (1992) Morphology of olfactory epithelium in humans and other vertebrates. Microsc Res Tech 23:49-61.

Mouly AM, Gervais R, Holley A (1990) Evidence for the involvement of rat olfactory bulb in processes supporting long-term olfactory memory. Eur J Neurosci 2:978-984.

Mouly AM, Kindermann U, Gervais R, Holley A (1993) Involvement of the olfactory bulb in consolidation processes associated with long-term memory in rats. Behav Neurosci 107:451-457.

Nusser Z, Kay LM, Laurent G, Homanics GE, Mody I (2001) Disruption of GABA(A) receptors on GABAergic interneurons leads to increased oscillatory power in the olfactory bulb network. J Neurophysiol 86:2823-2833.

Oka Y, Omura M, Kataoka H, Touhara K (2004) Olfactory receptor antagonism between odorants. Embo J 23:120-126.

Pinching AJ, Powell TP (1971) The neuropil of the glomeruli of the olfactory bulb. J Cell Sci 9:347-377.

Pressler RT, Strowbridge BW (2006) Blanes cells mediate persistent feedforward inhibition onto granule cells in the olfactory bulb. Neuron 49:889-904.

Ravel N, Chabaud P, Martin C, Gaveau V, Hugues E, Tallon-Baudry C, Bertrand O, Gervais R (2003) Olfactory learning modifies the expression of odour-induced oscillatory responses in the gamma (60-90 Hz) and beta (15-40 Hz) bands in the rat olfactory bulb. Eur J Neurosci 17:350-358.

Restrepo D, Miyamoto T, Bryant BP, Teeter JH (1990) Odor stimuli trigger influx of calcium into olfactory neurons of the channel catfish. Science 249:1166-1168.

Rochefort C, Gheusi G, Vincent JD, Lledo PM (2002) Enriched odor exposure increases the number of newborn neurons in the adult olfactory bulb and improves odor memory. J Neurosci 22:2679-2689.

Roskies AL (1999) The binding problem. Neuron 24:7-9, 111-125.

Rospars JP, Lansky P, Duchamp-Viret P, Duchamp A (2000) Spiking frequency versus odorant concentration in olfactory receptor neurons. Biosystems 58:133-141.

Roux SG, Garcia S, Bertrand B, Cenier T, Vigouroux M, Buonviso N, Litaudon P (2006) Respiratory cycle as time basis: an improved method for averaging olfactory neural events. J Neurosci Methods 152:173-178.

Rubin DB, Cleland TA (2006) Dynamical mechanisms of odor processing in olfactory bulb mitral cells. J Neurophysiol 96:555-568.

Schoenfeld TA, Cleland TA (2005) The anatomical logic of smell. Trends Neurosci 28:620-627.

Schoenfeld TA, Cleland TA (2006) Anatomical contributions to odorant sampling and representation in rodents: zoning in on sniffing behavior. Chem Senses 31:131-144.

Schoppa NE (2006a) A novel local circuit in the olfactory bulb involving an old short-axon cell. Neuron 49:783-784.

Schoppa NE (2006b) Synchronization of olfactory bulb mitral cells by precisely timed inhibitory inputs. Neuron 49:271-283.

Schoppa NE, Kinzie JM, Sahara Y, Segerson TP, Westbrook GL (1998) Dendrodendritic inhibition in the olfactory bulb is driven by NMDA receptors. J Neurosci 18:6790-6802.

Serizawa S, Ishii T, Nakatani H, Tsuboi A, Nagawa F, Asano M, Sudo K, Sakagami J, Sakano H, Ijiri T, Matsuda Y, Suzuki M, Yamamori T, Iwakura Y, Sakano H (2000) Mutually exclusive expression of odorant receptor transgenes. Nat Neurosci 3:687-693.

Song S, Miller KD, Abbott LF (2000) Competitive Hebbian learning through spike-timing-dependent synaptic plasticity. Nat Neurosci 3:919-926.

Spors H, Wachowiak M, Cohen LB, Friedrich RW (2006) Temporal dynamics and latency patterns of receptor neuron input to the olfactory bulb. J Neurosci 26:1247-1259.

Stopfer M, Jayaraman V, Laurent G (2003) Intensity versus identity coding in an olfactory system. Neuron 39:991-1004.

Stopfer M, Bhagavan S, Smith BH, Laurent G (1997) Impaired odour discrimination on desynchronization of odour-encoding neural assemblies. Nature 390:70-74.

Strotmann J, Conzelmann S, Beck A, Feinstein P, Breer H, Mombaerts P (2000) Local permutations in the glomerular array of the mouse olfactory bulb. J Neurosci 20:6927-6938.

Tozaki H, Tanaka S, Hirata T (2004) Theoretical consideration of olfactory axon projection with an activity-dependent neural network model. Mol Cell Neurosci 26:503-517.

Treisman A (1999) Solutions to the binding problem: progress through controversy and convergence. Neuron 24:105-110, 111-125.

Troemel ER, Chou JH, Dwyer ND, Colbert HA, Bargmann CI (1995) Divergent seven transmembrane receptors are candidate chemosensory receptors in C. elegans. Cell 83:207-218.

van Drongelen W, Holley A, Doving KB (1978) Convergence in the olfactory system: quantitative aspects of odour sensitivity. J Theor Biol 71:39-48.

Wellis DP, Scott JW (1990) Intracellular responses of identified rat olfactory bulb interneurons to electrical and odor stimulation. J Neurophysiol 64:932-947.

White J, Hamilton KA, Neff SR, Kauer JS (1992) Emergent properties of odor information coding in a representational model of the salamander olfactory bulb. J Neurosci 12:1772-1780.

Willhite DC, Nguyen KT, Masurkar AV, Greer CA, Shepherd GM, Chen WR (2006) Viral tracing identifies distributed columnar organization in the olfactory bulb. Proc Natl Acad Sci U S A 103:12592-12597.

Wilson DA, Leon M (1988) Spatial patterns of olfactory bulb single-unit responses to learned olfactory cues in young rats. J Neurophysiol 59:1770-1782.

Wilson DA, Stevenson RJ (2006) Learning to smell: olfactory perception from neurobiology to behavior. Baltimore: The Johns Hopkins University Press.

Xiong W, Chen WR (2002) Dynamic gating of spike propagation in the mitral cell lateral dendrites. Neuron 34:115-126.

Yokoi M, Mori K, Nakanishi S (1995) Refinement of odor molecule tuning by dendrodendritic synaptic inhibition in the olfactory bulb. Proc Natl Acad Sci U S A 92:3371-3375.

Yuan Q, Harley CW, McLean JH (2003) Mitral cell beta1 and 5-HT2A receptor colocalization and cAMP coregulation: a new model of norepinephrine-induced learning in the olfactory bulb. Learn Mem 10:5-15.

Zaborszky L, Carlsen J, Brashear HR, Heimer L (1986) Cholinergic and GABAergic afferents to the olfactory bulb in the rat with special emphasis on the projection

neurons in the nucleus of the horizontal limb of the diagonal band. J Comp Neurol 243:488-509.

Zufall F, Leinders-Zufall T (2000) The cellular and molecular basis of odor adaptation. Chem Senses 25:473-481.

Figure legends

Figure 1. Olfactory sensory neuron morphology. **A.** Scanning electron micrograph of the sensory surface of the human olfactory epithelium, showing the protruding dendritic knob and sensory cilia of an OSN. The microvilli of sustentacular (supporting) cells surround the OSN. **B.** Scanning electron micrograph of a fractured human olfactory epithelium in cross-section, showing an olfactory sensory neuron (OSN) surrounded by sustentacular cells. The columnar sustentacular cells extend the full depth of the epithelium. The OSN axon extends down and to the left, towards the cribriform plate and olfactory bulb. Micrographs courtesy of Richard M. Costanzo, Virginia Commonwealth University.

Figure 2. Illustration of a mechanism by which neurons expressing metabotropic receptors such as ORs can achieve arbitrarily high sensitivities (EC_{50}) to those receptors' ligands irrespective of their binding affinities (dissociation constant, K_d). Other terminology depicted is that of Cleland and Linster (1999). **A.** *Left panel.* If twice the number of receptors are expressed as are necessary to maximally activate the existing population of effector channels in a given neuron, the dissociation constant is unaffected and ligand-receptor binding over the level of maximum effector activation (1.0) has no further effect. *Center panel*. The dose-response curve then measured in that neuron would be cut off at the level of maximum effector activation. *Right panel*. Fitting this cut-off curve to a sigmoid yields an half-activation concentration (EC_{50}) that is lower than the dissociation constant, and this difference increases in proportion to the overexpression of receptors with respect to effectors (or, equivalently, to the effective gain of the intracellular G-protein

cascade). The abscissa represents ligand concentration as in B. **B.** A convergent population of neurons, such as OSNs, that each express a different (or loosely regulated) degree of receptor overexpression or intracellular gain will generate correspondingly different activation curves (each as in A, *center panel*). The summation of their output produces a collective dose-response curve (*sigmoid curve*) that is broader than any of those of the individual converging neurons, as is observed in the collective responses of OSNs visualized in glomerular imaging studies. Figures adapted from Cleland and Linster (1999).

Figure 3. Olfactory bulb circuit architecture. **A.** Illustration of major olfactory bulb circuit elements. OSN input arises from the bottom and forms excitatory synapses (*filled triangles*) onto mitral (Mi), periglomerular (PG), and external tufted (ET) cells. External tufted cells in turn excite PG cells, short-axon (SA) cells, and each other. Periglomerular cells inhibit mitral cell apical dendrites via $GABA_A$-mediated shunt inhibition (*open circles*) and OSN axon terminals via $GABA_B$ and dopamine D2 presynaptic receptors (*small open circles*). Mitral cell lateral dendrites extend along the external plexiform layer (EPL) and form reciprocal synapses with the dendritic spines of inhibitory granule cells (Gr), delivering recurrent inhibition onto themselves and lateral inhibition onto the lateral dendrites of other mitral cells. SA cells are not affiliated with any given glomerulus, but extend between them, forming a lateral excitatory network in the deep glomerular layer (Aungst et al., 2003; Cleland et al., 2007). Lower case labels denote incoming processes originating in other glomeruli. The *shaded area* connotes the approximate physical boundaries of the visible glomerulus. The *dotted box* connotes the column of neurons

associated with a particular glomerulus; the lower, glomerular layer (GL) section of the box contains the circuitry associated with the first, slow-timescale stage of OB processing, whereas the upper section contains the circuitry associated with the second, dynamical stage of processing. Middle/deep tufted cells and (deep) Blanes cells have been omitted for clarity. Olfactory bulb layers, surface to deep: *GL*, glomerular layer; *EPL*, external plexiform layer; *MCL*, mitral cell layer; *IPL*, internal plexiform layer; *GCL*, granule cell layer. **B.** Close-up rendition of the OSN-PG-mitral cell synaptic triad in the OB glomerulus. OSN axon terminals concomitantly excite mitral cell apical dendrites and periglomerular cell spines (*aka* gemmules); the excited periglomerular spines then deliver inhibition onto those same mitral cell dendrites (Pinching and Powell, 1971). Periglomerular cells also deliver $GABA_B$-ergic and dopamine D2 presynaptic inhibition onto OSN terminals.

Figure 4. Illustration of non-topographical contrast enhancement (NTCE) using a computational model based on the synaptic triad circuit in the OB glomerular layer (Figure 3B). **Ai-Aiv**. Odor-evoked activity in model mitral cells as a function of odor ligand-receptor affinity, in the absence of periglomerular inhibition and neglecting stimulus concentration. Increasing odor ligand-receptor affinity generates a monotonic increase in mitral cell activation. **Av-Aviii.** The addition of periglomerular inhibition upon local mitral cells creates a contrast enhancement generator element by first inhibiting (panel *vii*), and then exciting (panels *vi, v*), mitral cells as odor ligand-receptor affinity increases. Inhibition was held constant, and panels *v-viii* depict the same four odor ligand-receptor affinities as are shown in panels *i-iv*. **Aix-Ax.** Periglomerular cell activation by the two

lower-affinity odorant stimuli. While the depolarizing current input to periglomerular and mitral cells is identical, the greater input resistance and smaller volume of PG spines compared to mitral cell dendrites result in a greater voltage deflection in and hence a greater activation of PG cells (compare panels *iv* and *x*). Additionally, low-threshold T-type calcium current (McQuiston and Katz, 2001) evokes a near-maximal burst response from PG cells even at low input levels (panel *ix*), which mediates the mitral cell inhibition shown in panel *vii*. ***Inset.*** Model architecture. OSN synaptic input activates mitral cell apical dendrite, periglomerular dendritic spine, and a combined ET-SA-PG cascade that projects inhibition onto other mitral cells. *Filled triangles*: excitatory synapses. *Open triangles*: inhibitory synapses. *Lower case labels* denote incoming processes originating in other glomeruli. **B.** Spike count in a model mitral cell over a 1 sec stimulus in the absence and presence of PG cell-mediated NTCE, illustrating the NTCE half-hat function (Cleland and Sethupathy, 2006). In order to illustrate the effects of mitral cell inhibition, a 150 pA depolarizing current was continuously injected into the model mitral cell soma to elicit a baseline spike rate. Mitral cell spiking was employed solely as an index of activation as the model used did not include complex spike patterning mechanisms. With intact NTCE, the mitral cell activation level reflects a half-hat function as odor ligand-receptor affinity increases. **C.** Simplified theoretical model of the NTCE half-hat function depicted as the difference of two sigmoids. A principal neuron (mitral cell; Mi_{in}, *dashed line*) and a local inhibitory interneuron (periglomerular cell; PG, *dotted line*) are both directly, sigmoidally activated by increasing input levels (*abscissa*; here depicted as odorant-receptor affinity and neglecting odorant concentration). The local interneuron exhibits greater sensitivity to this input (i.e., it is half-activated by a weaker degree of odorant-receptor affinity owing,

for example, to its electrotonic compactness) while the larger principal neuron has a correspondingly greater maximum output amplitude. While input levels in a chemical binding context can conflate ligand-receptor affinity and ligand concentration, this ambiguity can be resolved by global feedback mechanisms (Cleland and Sethupathy, 2006; Cleland et al., 2007). When the two neurons are driven by the same input and the local interneuron inhibits the principal neuron, the net output activity of the principal neuron can become nonmonotonic with respect to input level, exhibiting a half-hat function capable of mediating contrast enhancement (mitral cell; Mi_{out}, *solid line*). That is, with respect to the receptive field of any glomerulus, the mitral cell output profile after NTCE (Mi_{out}) will exhibit a narrower selectivity for odorants than do its associated ORs (Mi_{in}). Figures adapted from Cleland and Sethupathy (2006).

Figure 5. Illustration of a dynamical mechanism for contrast enhancement mediated by spike timing-dependent plasticity (STDP; (Song et al., 2000)). The upper panels are aligned in time with their respective lower panels, which depict the effect of the STDP learning rule: presynaptic spikes that precede the postsynaptic spike that they help evoke are strengthened (with the most strongly potentiated synapse being that delivering the presynaptic spike most immediately preceding the postsynaptic spike; *black curve*), whereas presynaptic spikes that follow the evoked postsynaptic spike are weakened (*grey curve*). **A.** Response of a model cell activated by a weak stimulus. Six input spikes are accumulated before a spike is evoked in the model cell, such that six of the ten input synapses are strengthened to varying degrees (*black raster marks*) and four weakened (*grey raster marks*). **B.** Response of a model cell activated by a stronger stimulus (in

terms either of binding affinity or of concentration). Strong odor stimuli evoke oscillations of similar frequency but higher power (Stopfer et al., 2003), which has the effect of more tightly phase-constraining evoked spikes (Linster and Cleland, 2001; Cleland and Linster, 2002). The increased spike density (within the active phase of each cycle) evokes a postsynaptic spike after only three input spikes have accumulated, reducing the number of input synapses that are strengthened (*black*) and increasing the number that are weakened (*grey*). As the earlier spikes represent the responses of the neurons best-tuned to the stimulus presented (see text), this STDP-mediated learning process enhances the best-tuned input synapses and specifically targets the moderately-tuned inputs for weakening, generating a dynamical variant of the half-hat function. The implication for olfactory representation is that mitral cell spikes may occur that do not contribute to the determination of downstream neural activity, hence differentiating *effective activity* from *ineffective activity* in the mitral cell ensemble. In this dynamical regime of effective activity, tighter synchrony mediates narrower receptive fields.

Figure 1

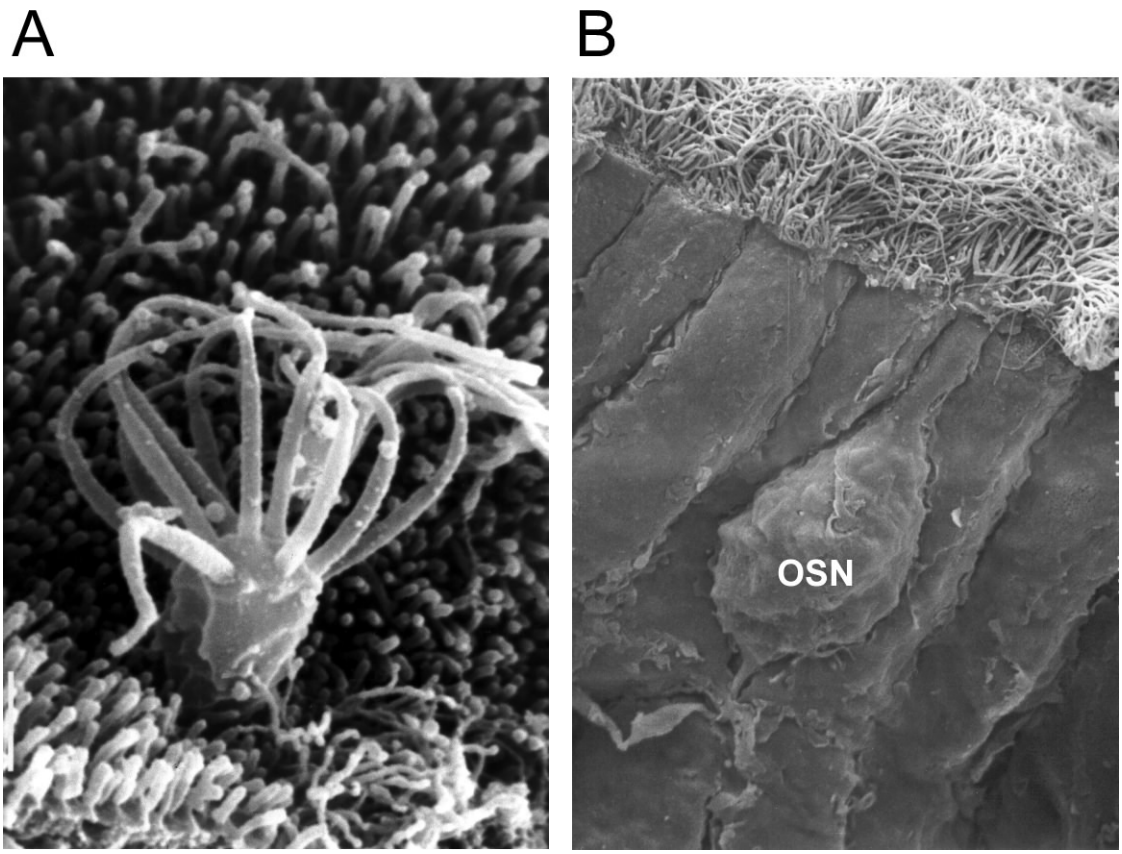

Figure 2

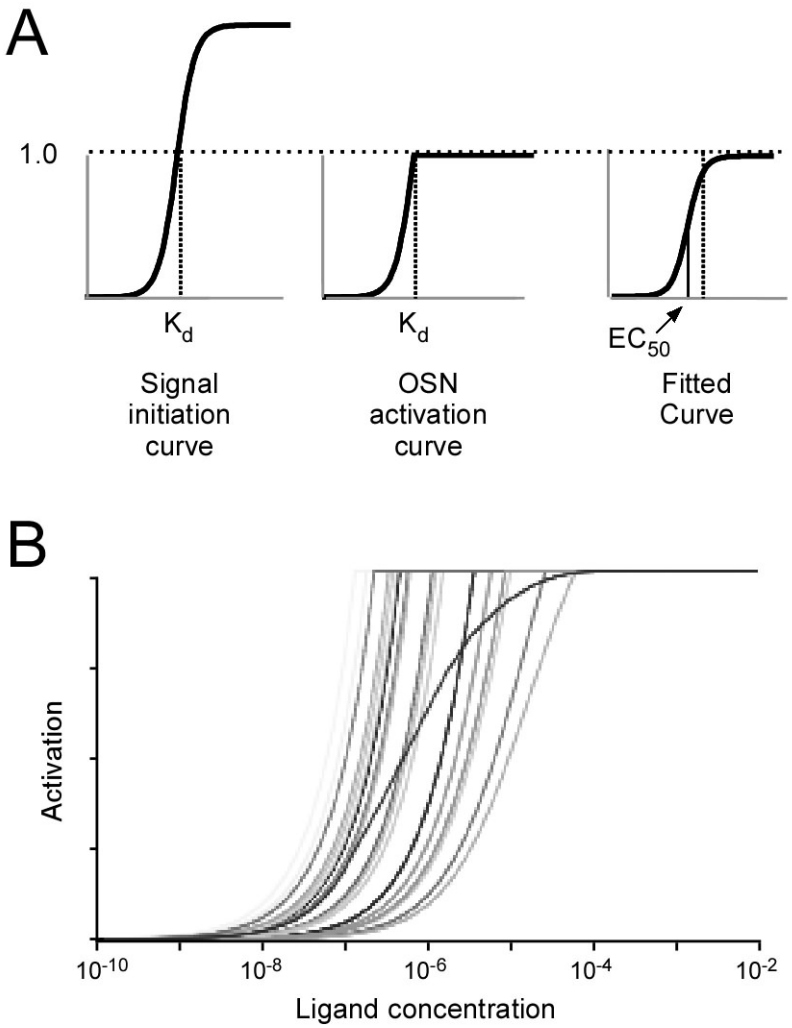
A
1.0
K_d
K_d
EC_{50}
Signal initiation curve
OSN activation curve
Fitted Curve
B
Activation
10^{-10}
10^{-8}
10^{-6}
10^{-4}
10^{-2}
Ligand concentration

Figure 3

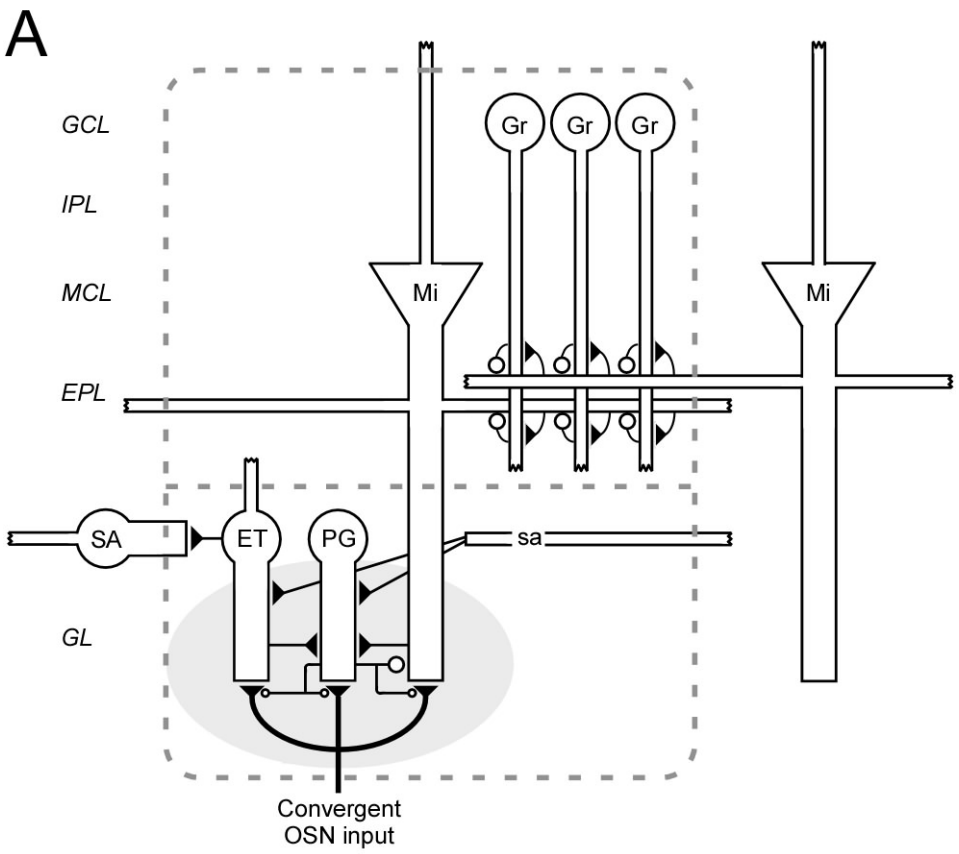
A
GCL
IPL
MCL
EPL
GL
Gr
Gr
Gr
Mi
Mi
SA
ET
PG
sa
Convergent
OSN input

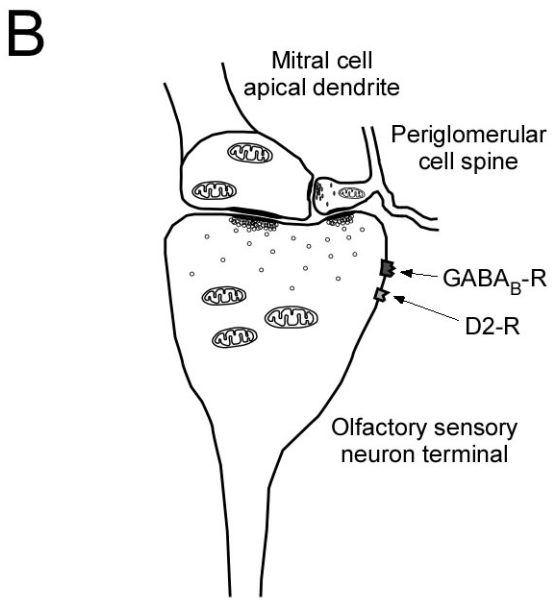
B
Mitral cell
apical dendrite
Periglomerular
cell spine
GABA$_B$-R
D2-R
Olfactory sensory
neuron terminal

Figure 4

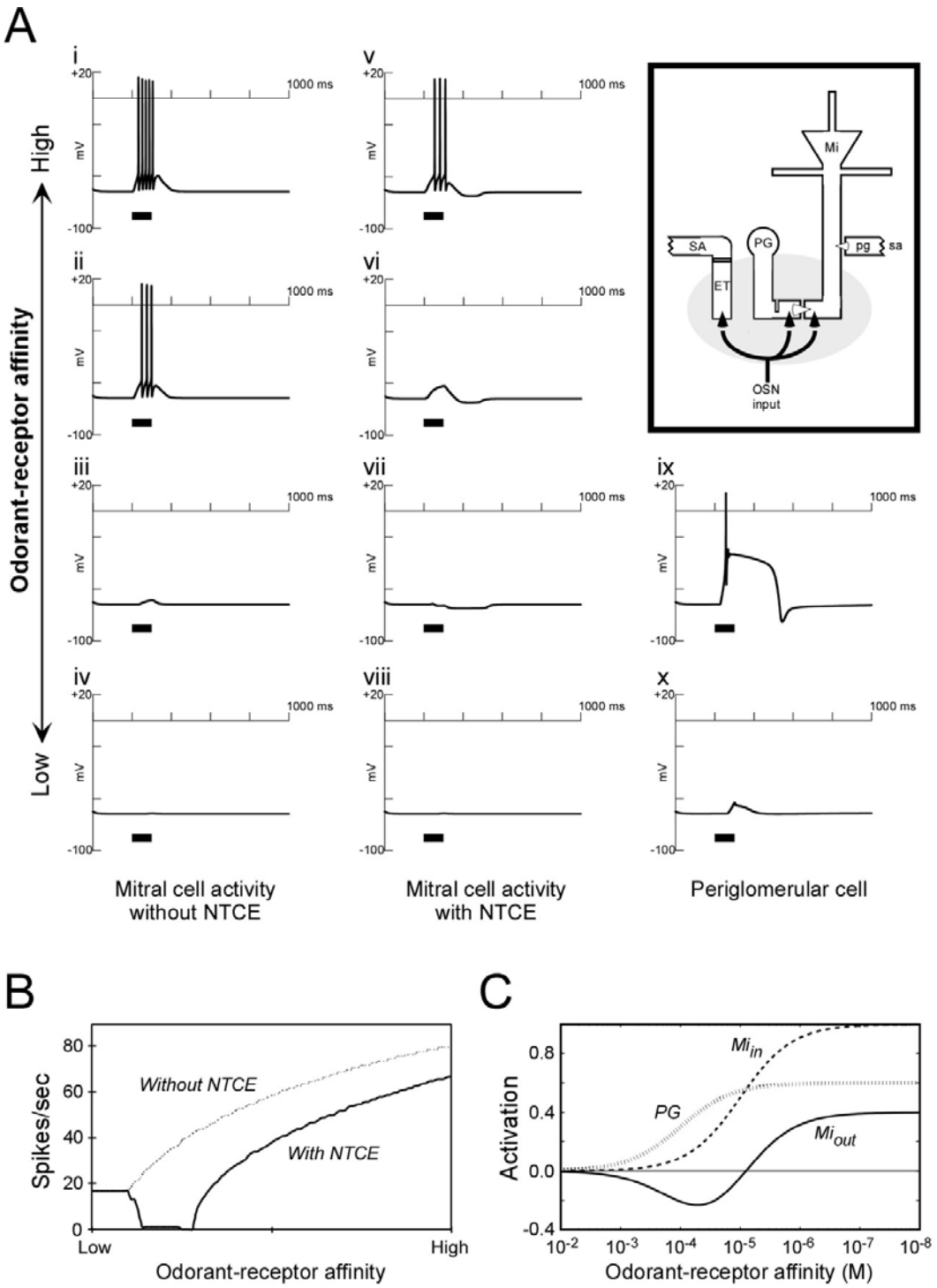
A
i
v
ii
vi
iii
vii
ix
iv
viii
x
+20
-100
mV
1000 ms
High
Low
Odorant-receptor affinity
Mi
SA
PG
pg
sa
ET
OSN
input
Mitral cell activity
without NTCE
Mitral cell activity
with NTCE
Periglomerular cell
B
Spikes/sec
80
60
40
20
0
Without NTCE
With NTCE
Low
High
Odorant-receptor affinity
C
Activation
0.8
0.4
0.0
-0.4
Mi_in
PG
Mi_out
10-2
10-3
10-4
10-5
10-6
10-7
10-8
Odorant-receptor affinity (M)

Figure 5